Measurement of pre- and post-fission neutron emission at moderate excitation energies*

Z. Fraenkel†
Argonne National Laboratory, Argonne, Illinois 60439
and Weizmann Institute of Science, Rehovot, Israel

I. Mayk
Weizmann Institute of Science, Rehovot, Israel

J. P. Unik, A. J. Gorski, and W. D. Loveland‡
Argonne National Laboratory, Argonne, Illinois 60439
(Received 9 June 1975)

Fission fragment mass-energy distributions and the coincident neutron velocity distributions have been measured at 0° and 90° with respect to the fragment direction. The fissioning systems studied were ^{209}Bi, ^{232}Th, ^{233}U, ^{238}U, and ^{239}Pu bombarded with 45 MeV α particles and ^{226}Ra bombarded with 16 MeV protons. From the above measured quantities the number of pre-fission neutrons and the number of post-fission neutrons were obtained as a function of fragment mass and total fragment kinetic energy. The average number of pre-fission neutrons emitted is 2.9 ± 0.9 for the ^{232}Th target, 3.3 ± 1.5 for ^{233}U, 3.6 ± 1.6 for ^{238}U, and 2.7 ± 0.8 for ^{239}Pu. The average number of post-fission neutrons emitted by these systems is 4.4 ± 0.3, 4.2 ± 0.7, 4.6 ± 0.7, and 5.1 ± 0.3, respectively. (The values reported for pre-fission neutrons include also contributions from scission neutrons.) The number of pre-fission neutrons from the ^{226}Ra + 16 MeV proton system is 0.5 ± 0.3. The number of post-fission neutrons is 3.6 ± 0.4. The number of neutrons emitted from the ^{209}Bi + 45 MeV α particle system is 3.6 ± 0.2. The number of post-fission neutrons as a function of fragment mass and total kinetic energy which were obtained by the direct neutron measurements of this work are lower and are more consistent with calculated total energy balances than the values obtained by the indirect method based on the simultaneous measurement of both the kinetic energy and the velocity of the fission fragments. Our results for the average number of pre-fission neutrons are compared with calculations based on the conventional expression for Γ_f/Γ_n. The agreement between the calculated results and our experimental results is satisfactory. However, the calculations predict spallation cross sections which are much larger than those obtained experimentally by radiochemical methods.

[NUCLEAR REACTIONS, FISSION ^{209}Bi(α, f), ^{232}Th(α, xnf), ^{233,238}U(α, xnf), ^{239}Pu(α, xnf), $E=45$ MeV; ^{226}Ra(p, xnf), $E=16$ MeV; measured coin. fragment energy, neutron velocity at $\theta=0°$, 90° with respect to fragment; deduced number of pre-fission, post-fission neutrons.]

I. INTRODUCTION

In recent years a number of studies[1-7] have been made of the dependence of the fission cross section σ_f of heavy elements on the properties of the fissioning system, in particular its mass, charge, excitation energy, and angular momentum. In addition to the fission cross section, convenient quantities for the comparison between various fissioning species are the fission width Γ_f and the ratio Γ_f/Γ_n (Γ_n is the neutron emission width) and the fission probability P_f. Since neutron emission is normally the only competing reaction, $P_f=\Gamma_f/(\Gamma_f+\Gamma_n)$. For light ($Z\lesssim 82$) systems at moderate excitation energies ($E^*\lesssim 50$ MeV), second chance fission (fission following emission of one neutron) can be ignored and Γ_f/Γ_n can be directly determined by obtaining the fission cross section and the total reaction cross section. This is in general not the case for heavy ($Z\geq 90$) nuclei where the probability for second chance fission is appreciable except at very low excitation energies. One indirect way of measuring Γ_f/Γ_n for these systems is the measurement of the average number of neutrons emitted prior to fission. A calculation of the fission-spallation competition, which is critically dependent on Γ_f/Γ_n must be able to reproduce, among other quantities, the average number of neutrons emitted before fission. However, such a comparison is complicated by the fact that Γ_f/Γ_n is a function of both the mass number A and the excitation energy E^* of the fissioning system and both these quantities change during the neutron evaporation stage preceding fission. For this reason most authors have confined their studies to elements lighter than $Z=90$[1-4,6] or to a limited range of excitation energies.[5]

Several years ago Cheifetz *et al.*[8] measured the

number of neutrons emitted before fission in the bombardment of ^{209}Bi and ^{238}U with 155 MeV protons. They were unable to obtain good agreement between their results and radiochemical results for spallation residues on one hand and the conventional theoretical expression[9,10] for $\Gamma_f/\Gamma_n(E^*)$ on the other hand. However, the interpretation of their results involves an additional complication since at these bombarding energies the so-called fission-spallation competition is preceded by a fast intranuclear cascade process.[9] During this stage of the reaction high energy protons and neutrons are emitted and because of its short time scale (~10^{-23} sec) fission is not believed to be a competing reaction. It is therefore of interest to repeat these measurements at lower bombarding energies (~50 MeV) where compound nucleus formation is the predominant first stage of the reaction. The probability of a fast intranuclear cascade is also reduced when α particles rather than protons are used as bombarding particles.

Our experimental arrangement and method of analysis were similar to those used by Cheifetz *et al.*[8] and are based on the experiment first performed by Harding and Farley[11]: The neutron energy spectrum is measured in coincidence with the two fission fragments at two or more angles (normally 0° and 90°) with respect to the direction of the fission fragments. The average number and energy spectrum of the pre-fission neutrons and of the post-fission neutrons can then be determined by an iteration process based on two assumptions: (1) The pre-fission neutrons are emitted isotropically in the center-of-mass (c.m.) system of the fissioning nucleus. (2) The post-fission neutrons are emitted isotropically in the c.m. system of the fully accelerated fragments. Both assumptions are not completely justified because of the angular momentum of the fissioning system and of the fragments. The magnitude of these latter effects will be briefly discussed below.

Our results for the pre-fission neutrons also include a contribution due to "scission" neutrons which are emitted during the transition of the fissioning nucleus from the saddle point to the scission point and during the scission process. They are generally assumed to be emitted isotropically in the c.m. frame of the fissioning system and hence cannot be separated by our method from the pre-fission neutrons which are emitted prior to the saddle-to-scission transition. Evidence for scission neutrons was found in the spontaneous fission of ^{252}Cf[12] and in the thermal-neutron fission of ^{235}U.[13] The emission of scission neutrons is also very likely in view of the emission of other light particles in the scission process.[14]

The analysis of the pre-fission and post-fission neutron distribution was similar to that of Cheifetz *et al.*[8] However, we did include a recoil correction for the post-fission neutrons.[15] This correction does not affect the average number of pre-fission and of post-fission neutrons but it decreases the variation of the average number of post-fission neutrons with the fragment mass number and total kinetic energy.

II. EXPERIMENTAL ARRANGEMENT

The experimental arrangement was designed to detect neutrons in coincidence with the two fission fragments in the fission induced in ^{209}Bi, ^{232}Th, ^{233}U, and ^{239}Pu by 45 MeV α particles from the ANL 152 cm cyclotron and in ^{226}Ra by 16 MeV protons from the ANL FN tandem. Since the fragment mass, kinetic energy, and the neutron velocity and angular distributions of the spontaneous fission of ^{252}Cf have been studied previously,[12,16] measurements with ^{252}Cf were also performed at convenient time intervals so as to provide the calibration of the fragment mass and kinetic energy measurements and the determination of the neutron detection efficiency as a function of neutron velocity.

Thin targets were placed in the beam direction in the center of a vacuum chamber. Inside the chamber, solid state detectors (SSDs) were positioned to detect the two complementary fission fragments. Outside the chamber, two plastic scintillators attached to photomultipliers detected the neutrons emitted. The delay between the signals of one of the fission detectors and the scintillation detector allowed the determination of the neutron time-of-flight (TOF). In addition, the amplitude of the photomultiplier signal was also measured and recorded. The random background in the TOF spectra was obtained by measuring events in which the scintillator signal preceded the fission signal.

In the ^{209}Bi experiment, two neutron detectors were positioned to detect neutrons emitted in the direction of the fragment detectors on opposite sides of the vacuum chamber. This arrangement was chosen for ^{209}Bi in order to double the counting rate in view of its relatively low fission cross section. It does not enable the separation between pre-fission and post-fission neutrons. However, second chance fission is negligible for this fissioning system.

In the ^{232}Th, ^{233}U, ^{238}U, and ^{239}Pu experiments one of the two scintillators was placed at 90° with respect to the fragment direction. This angle is optimal for pre-fission neutron detection since the post-fission neutron angular distribution has its minimum at this angle. The other scintillator was

placed at 0° with respect to one of the fragment detectors (detector No. 1).

In the ^{226}Ra experiment, the neutron velocity distribution was also measured at 0° and 90° with respect to the fragment direction. However, *two* pairs of fragment detectors were placed inside the vacuum chamber in a plane perpendicular to the beam direction and at 90° to each other. Hence, each scintillator was at 0° with one pair of SSDs and at 90° with respect to the other pair. This arrangement had the advantage of doubling the counting rate and measuring with each neutron detector the neutron velocity distribution at both 0° and 90° with respect to the fragment direction.

The thickness for the different targets is shown in Table I, together with the average energy loss of the fission fragments in the target itself, taking into account the target angle with respect to the fission fragment detector. All targets had a 45 μg/cm^2 Ni backing. Ni protection foils of the same thickness were used in front of the fission detectors.

In the cyclotron experiments we used a horizontal target chamber (i.e., its axis was at 90° to the beam axis) of 25 cm diameter and 0.5 cm Al wall thickness. In the tandem experiment we used a somewhat larger Al chamber of the same wall thickness but its axis coincided with the beam axis. The fission detectors were 4 cm^2 gold surface-barrier detectors. One detector of each pair (detector No. 1) was placed at a distance of 5 cm from the target and it determined the solid angle of the fission fragment detection system whereas the other detector (detector No. 2) was placed at a distance of 4 cm from the target. In the cyclotron experiment each of the fission fragment detectors was placed at angle of 3.5° (downstream) with respect to the plane perpendicular to the beam in order to compensate for the recoil momentum of the compound nucleus. No such correction was necessary in the tandem experiment. Due to the finite size of the beam and the angular spread of the fission fragments resulting from neutron emission, only ~85% of the fission events in the angle-defining detector (No. 1) were coincidence events.

The neutron detector consisted of an NE 102 plastic scintillator of 2 cm thickness and 12.5 cm diameter mounted on an 58 AVP photomultiplier. The face of the scintillator was at a distance of 50 cm from the center of the chamber.

The pulse from each fission detector was fed in parallel to a time-pickoff unit and to a charge sensitive preamplifier followed by an amplifier. The fast signals from the time-pickoff units were used for a fast coincidence between the pulses of each pair of fission detectors and the fast signal from detector No. 1 was used as a start signal for the time-to-amplitude converter (TAC) which measured the neutron flight time. Pulses from the anode of the photomultiplier (PM) were fed to a fast discriminator, the output of which served as a stop signal for the TAC. In addition, the analog signal from the PM was fed into a conventional amplifier. The output signals from the TAC and the amplifiers of the fission detectors and PM analog pulses were fed into a four-dimensional analyzer and recorded sequentially on magnetic tape.

III. DATA ANALYSIS

A. Determination of the mass and kinetic energy of the fission fragments

The kinetic energies of the fission fragments were obtained from the pulse heights of the solid state detectors by the calibration procedure of Schmitt, Kiker, and Williams.[17]

The recoil energy of the compound nucleus of mass number A prior to pre-fission neutron emission is $E_{\text{recoil}} = (m_0/A)E_{\text{lab}}$ where m_0 is the projectile mass number and E_{lab} is the bombarding energy. The values of E_{recoil} are shown in Table I. The recoil correction for the fragment m_1 is $\Delta E = (m_1/A)E_{\text{recoil}}$. ($m_1$ is the post-neutron-emission mass.) The determination of the fragment mass values is insensitive to this correction since they are a function of the fragment kinetic energy *ratio*. The main effect of this correction is to shift the total fragment energy by E_{recoil}.

The pre-neutron emission fragment masses M_1 and total kinetic energies E_K were determined by an iterative process similar to that described by Watson *et al.*[18] Since the iterations also require the knowledge of the average number of pre-fission neutrons $\bar{\nu}_b$ and the average number of post-fission neutrons as a function of fragment mass and kinetic energy $\bar{\nu}_1(E_K, M_1)$, the calculation of these quantities must be included in the iteration. In the first iteration we assumed $\bar{\nu}_1(E_K, M_1)$ to be zero. In later iterations the matrix $\bar{\nu}_1(E_K, M_1)$ was smoothed using a three-point interpolation procedure. For sake of simplicity we assumed $\bar{\nu}_b = 0$ for the ^{209}Bi + α and ^{226}Ra + p systems and $\bar{\nu}_b = 3$ for the highly fissile systems.

B. Neutron recoil correction

If a post-fission neutron is detected in coincidence with the fragment from which it was emitted, an additional correction must be made to the fragment kinetic energy as the result of the recoil momentum imparted to it by the neutron.[15] This correction is (to first order in M_1^{-1})

$$\Delta E_n = -\frac{2E_1}{M_1}\left(\frac{v}{V_1}\cos\theta - 1\right), \quad (1)$$

where V_1 and v are the laboratory velocities of the fragment and the neutron, respectively, and θ is the laboratory angle between the fragment and neutron detector.

In practice we do not know from which of the two fragments the neutron was emitted. Moreover, for the highly fissile systems the neutron may also be a pre-fission neutron in which case the correction to the fragment energy is (to first order)

$$E_n = -\frac{2E_1}{A}\frac{v}{V_1}\cos\theta, \quad (2)$$

where A is the mass number of the compound nucleus.

In our analysis we assumed: (1) that a neutron detected at $\theta = 0°$ with respect to a fission fragment was emitted from that fragment and applied the appropriate correction [Eq. (1)] to the fragment kinetic energy; (2) that neutrons detected at 90° with respect to the fission fragment direction were pre-fission neutrons and hence, applied no correction to the fragment energies in this case [see Eq. (2) for $\theta = 90°$]. Based on our results for the number of pre- and post-fission neutrons, we estimate that we applied the right correction in 70–80% of the events in which neutrons were detected at 0° in the case of the highly fissile systems (this number is higher for the ^{226}Ra and ^{209}Bi experiments) and in 60–80% of the events in which neutrons were detected at 90° with respect to the fission axis. Since this correction amounts, at most, to a few MeV, its main effect is on the variation of the number of neutrons with mass $\nu_1(M)$ and on $\partial\nu_1/\partial E_K(M)$ and to a lesser extent on the fragment masses.[15]

TABLE I. The target, projectile, compound nucleus, bombarding energy E_{lab}, excitation energy of the compound nucleus E^* and its recoil energy E_{recoil}, the target thickness, and the average fragment energy loss in the target ΔE for the fissioning systems studied in the present work.

Target	^{209}Bi	^{226}Ra	^{232}Th	^{233}U	^{238}U	^{239}Pu
Projectile	α	p	α	α	α	α
Compound nucleus	^{213}At	^{227}Ac	^{236}U	^{237}Pu	^{242}Pu	^{243}Cm
E_{lab} (MeV)	45	16	45	45	45	45
E^* (MeV)	34.9	21.0	39.7	38.5	39.3	38.1
E_{recoil} (MeV)	0.85	0.07	0.77	0.76	0.75	0.74
Thickness (μg/cm^2)	100	50	30	20	20	20
ΔE (MeV)	0.8	0.6	0.3	0.2	0.2	0.2

C. Neutron velocity distribution

1. Time-of-flight measurement

The neutron time-of-flight (TOF) T_n consists of the contribution of four terms

$$T_n = t_0 + t_r + t_f + t_n, \quad (3)$$

where t_0 is a fixed time interval determined by the detectors and the subsequent electronic circuits. t_r is the time delay associated with the rise time of the fission detector pulse which served as start pulse for the time-to-amplitude converter (TAC). We assumed t_r to be a linear function of the fragment energy E_1, $t_r = \beta E_1$. β was extracted from the time difference in the γ peak for distant mass and energy events ($\beta = -0.015 \pm 0.005$ nsec/MeV). t_f is the time of flight of the fragment to detector No. 1 which initiated the TAC start pulse $t_f = d/V_1$, where d is the distance from the target to detector No. 1 and V_1 is the fragment velocity. t_n is the measured time difference between the start pulse initiated by the fission fragment in detector No. 1 and the stop pulse initiated by the neutron upon being detected in the neutron detector, i.e., it is the time measured by the TAC system. $t_n = gI$ where I is the pulse amplitude generated by the TAC and g is the TAC calibration constant (for our system $g \cong 0.25$ nsec/channel).

The relative resolution of the TOF system is given by

$$\frac{\Delta v}{v} = \frac{1}{\bar{D}}[(\Delta t v)^2 + (\Delta D)^2]^{1/2}, \quad (4)$$

where $\bar{D}$ is the average distance traversed by the neutron before being detected, ΔD is the spread in the distance D due to the finite thickness of the scintillator, and Δt is the time spread of the electronic system. For the neutron velocity range of 1.0–4.5 cm/nsec we have

$$1.29 < \Delta D(\text{FWHM}) < 1.37 \text{ cm}.$$

Δt may be obtained from the experimental width of the γ peak in the TOF spectrum. A value of $\Delta t = 1.5$ nsec [full width at half-maximum (FWHM)] was obtained consistently throughout the experiment. The relative resolution of the TOF system for the above velocity range is therefore

$$0.04 < \frac{\Delta v}{v}(\text{FWHM}) < 0.14.$$

The large uncertainty for the high-velocity end of the neutron spectrum is offset by the small statistical weight of this velocity range.

2. Subtraction of random events

We used the TOF spectrum of a beam period preceding the correct interval to subtract the ran-

dom events from the relevant velocity interval. Fortunately there was no time structure in the random event interval which corresponded to the time interval of interest ($v = 1.0-4.5$ cm/nsec), i.e., the random events presented a constant background which could be readily subtracted.

D. Effective neutron detection efficiency

The measurement of the effective neutron detection efficiency of our system was based on the neutron density distribution $\rho(v, \theta)$ for the spontaneous fission of ^{252}Cf which has been determined by Bowman *et al.*[12] The number of neutrons in the velocity interval v to $v + \Delta v$ detected per steradian at an angle θ with respect to the fission axis in coincidence with the fission fragments in a given time interval is

$$N(v, \theta) = N_0 \epsilon(v) \rho(v, \theta) v^2 \Delta v \,, \tag{5}$$

where N_0 is the total number of fission events detected in the time interval and $\epsilon(v)$ the neutron detection efficiency. We measured $N(v, \theta)$ for ^{252}Cf at $\theta = 0°$, 90° at regular intervals during our experiment. This was done by inserting into the vacuum chamber a ^{252}Cf source instead of a target but leaving the rest of the experimental system unchanged. Using the $\rho(v, \theta)$ values of Bowman *et al.*, we thus were able to extract $\epsilon(v)$ for our detection system. The efficiency so obtained has the advantage of being an *effective* efficiency for our system, which already includes first-order corrections due to neutron elastic and inelastic scattering and $(n, n'\gamma)$ reactions. (This matter is described in greater detail by Cheifetz *et al.*[8]) It has the disadvantage that as a result of the anisotropy of $\rho(v, \theta)$, the scattering corrections vary with the detection angle θ and with the fissioning system and bombarding energy. Hence, the *effective* detection efficiency is angle dependent and the function $\epsilon_i(v, \theta)$ obtained for ^{252}Cf will not be strictly correct for other fissioning species.

Bowman *et al.*[12] tabulated $\rho(v, \theta_L)$ for ^{252}Cf in the angular range $\theta_L = 11.25-168.75°$ where θ_L is the angle with respect to the light fragment. In order to avoid errors due to the incorrect identification of the fragments in the symmetric mass region, we did not differentiate between light and heavy fragments in our measurement of $N(v, \theta)$ of ^{252}Cf and used $[\rho(v, \theta_L) + \rho(v, \pi - \theta_L)]$ of Bowman *et al.* for obtaining $\epsilon_i(v, \theta)$. Since the values of Bowman *et al.* do not extend to $\theta = 0$ and 180°, we extrapolated their values by fitting them to a 10th-order Legendre polynomial. The expansion coefficients were corrected for the finite size of the neutron and fragment detectors in a manner described by Rose.[19]

The theoretical neutron detection efficiency $\epsilon_T(v)$ may be readily calculated if we restrict ourselves to a single n-p scattering of the neutron in the scintillator. This approximation is valid if the mean free path of the neutron $\lambda(v)$ is long compared to the scintillator thickness h. In our experimental $0.1 < h/\lambda(v) < 0.6$. Hence, the approximation is valid for the high-velocity end of the spectrum and yields a lower bound for $\epsilon_T(v)$ at the low-velocity end.

We show in Figs. 1 and 2 the effective efficiency $\epsilon_i(v, \theta)$ for $\theta° = 0$ and 90°, respectively, as well as the theoretical efficiency $\epsilon_T(v)$. $\epsilon_i(v, \theta = 0°)$ and $\epsilon_T(v)$ agree very well above $v = 2$ cm/nsec. The lower values of $\epsilon_i(v, \theta = 0)$ for the low-velocity end are probably due to experimental threshold effects. The better agreement of $\epsilon_i(v, \theta = 90°)$ at the low-velocity end is fortuitous and is due to scattering and background effects which are more serious at this angle. The discrepancy in $\epsilon_i(v, 90°)$ at the high-velocity end will be discussed below.

The effective efficiency $\epsilon_i(v, 90°)$ obtained from the ^{252}Cf results is an upper limit for the true efficiency at this angle. The number of ^{252}Cf events detected at any angle θ may be written

$$N_i(v, \theta) = N_{id}(v, \theta) + N_{is}(v, \theta),$$

where $N_{id}(v, \theta)$ refers to neutrons which were emitted in the θ direction and did not undergo any scattering and $N_{is}(v, \theta)$ refers to all other events detected at this detector angle ("scattered" events). In the following i refers to the ^{252}Cf results and j to the detection efficiency for a different fissioning system. We have

$$\epsilon_j(v, \theta) \cong \frac{p_i(v, \theta)}{p_j(v, \theta)} \epsilon_i(v, \theta) \,, \tag{6}$$

where $p_i = N_{id}(v, \theta)/N_i(v, \theta)$ and similarly for p_j. Since the scattering effect is very small at $\theta = 0°$ (see next section) we have at this angle $(1 - p_i)$, $(1 - p_j) \ll 1$ and $\epsilon_j(v, 0°) \simeq \epsilon_i(v, 0°)$.

The scattering effect is largest at $\theta = 90°$ since there the number of "direct" events N_d is smallest and the correction is largest for ^{252}Cf for which the number of pre-fission neutrons (neglecting "scission neutrons") is zero, i.e., $p_i(v, 90°) \leq p_j(v, 90°)$ where i again refers to ^{252}Cf and j to all other fissioning systems. We therefore have

$$\epsilon_j(v, 90°) \leq \epsilon_i(v, 90°).$$

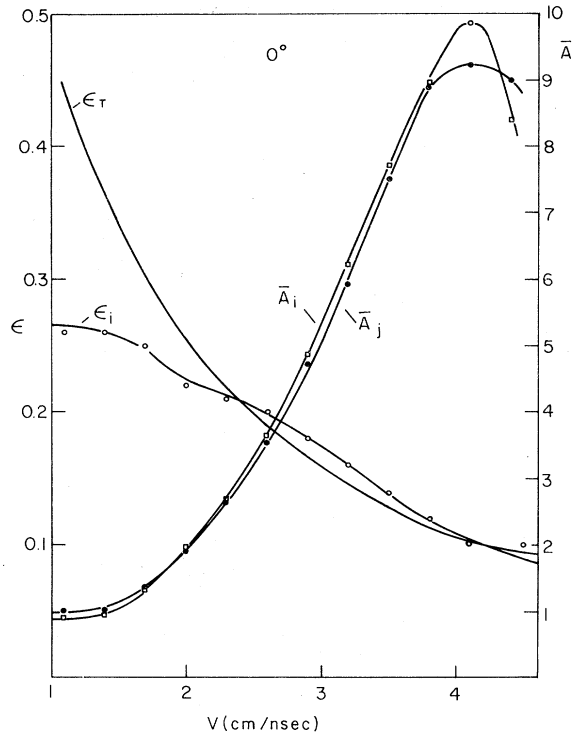

FIG. 1. The measured effective efficiency $\epsilon_i(v)$ and the theoretical efficiency $\epsilon_T(v)$ as a function of the neutron velocity v at $\theta = 0°$. Also shown are the average neutron detector pulse height parameters $\bar{A}_j(v)$ and $\bar{A}_i(v)$ obtained for the fissioning system being measured (^{232}Th + 45 MeV α particles) and for the calibration system (^{252}Cf), respectively, at the same angle.

E. Neutron pulse height parameter

As was mentioned above we recorded, in addition to the neutron TOF, the pulse heights produced in the neutron detectors. We show in Figs. 1 and 2 the average pulse height $\bar{A}(v)$ associated with an event in which a neutron of velocity v was detected. As before the subscript i refers to the ^{252}Cf results, whereas the subscript j refers in this particular case to the ^{232}Th + α results. It is seen that at 0° (Fig. 1) the two curves $A_i(v)$ and $A_j(v)$ are very similar. In view of the fact that the number of neutrons per fission and their angular distribution in the laboratory system is very different, the similarity of the $\bar{A}(v)$ curves may be taken as a proof that the scattering effects are negligible at this angle and $\epsilon_i(v)$ obtained at this angle is essentially the "true" detection efficiency.

The average pulse heights $A(v)$ for ^{252}Cf (subscript i) and ^{232}Th + α (subscript j) at $\theta = 90°$ (Fig. 2) differ quite substantially at the high velocity region. Whereas $\bar{A}_j(v, 90°)$ is very similar to the $\bar{A}_j(v, 0°)$ curve (indicating that the scattering correction for the ^{232}Th + α system is also small at 90°), the average pulse height for ^{252}Cf, $A_i(v, \theta)$, is substantially lower for high v. This may indicate an insufficient separation of the γ and neutron peaks or a substantial contribution of $(n, n'\gamma)$ scattering events in which the γ ray was detected.

The neutron pulse height curves $\bar{A}_i(v)$ and $\bar{A}_j(v)$ may be used to obtain a better upper limit for the effective efficiency at $\theta = 90°$. Using the same notation as in the previous section we may write

$$\bar{A}_i(v, \theta) = p_i(v, \theta)\bar{A}_{id}(v, \theta) + [1 - p_i(v, \theta)]\bar{A}_{is}(v, \theta)$$

and a similar equation holds for $\bar{A}_j(v, \theta)$. We have

$$\bar{A}_{id}(v, \theta) = \bar{A}_{jd}(v, \theta)$$

and we make the assumption

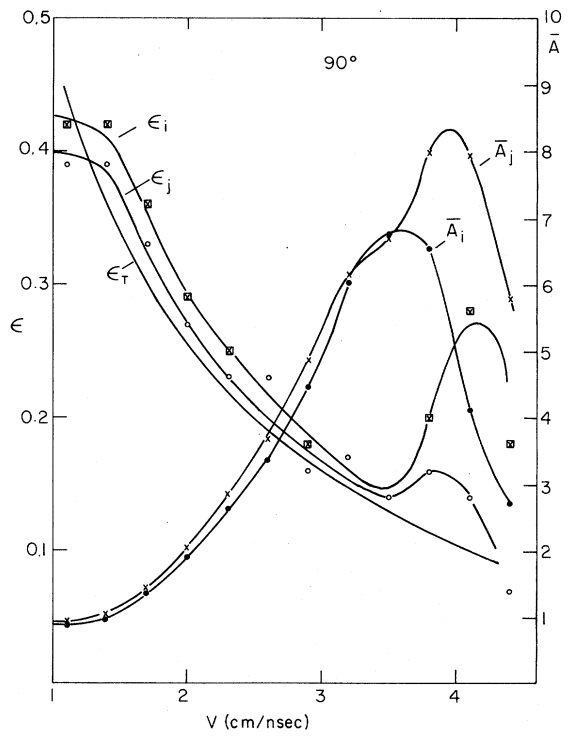

FIG. 2. The effective efficiencies $\epsilon_j(v)$ and $\epsilon_i(v)$ for the fissioning system being measured (^{232}Th + 45 MeV α particles) and for the calibration system (^{252}Cf), respectively, and the theoretical efficiency $\epsilon_T(v)$ as a function of the neutron velocity at 90°. Also shown are the respective average neutron detector pulse height parameters $\bar{A}_j(v)$ and $\bar{A}_i(v)$ at this angle.

$$\bar{A}_{is}(v,\theta)=\bar{A}_{js}(v,\theta)\,,$$

i.e., the "scattered" events give the same average pulse height for all fissioning systems. With the further assumption $p_i(90°)\leq p_j(90°)$ (i – ^{252}Cf events), it follows that

$$\frac{\bar{A}_i(v,90°)}{\bar{A}_j(v,90°)}\geq\frac{p_i(v,90°)}{p_j(v,90°)}\,.$$

Using Eq. (6) we have finally

$$\epsilon_j(v,90°)\leq\frac{\bar{A}_i(v,90°)}{\bar{A}_j(v,90°)}\epsilon_i(v,90°) \tag{7}$$

which is a better upper limit for $\epsilon_j(v)$ at 90°. The upper limit for $\epsilon_j(v)$ obtained from Eq. (7) for ^{232}Th + α is also shown in Fig. 2. It is seen that the "anomalous" peak at the high-velocity end is substantially reduced with this correction. Similar curves $\epsilon_j(v,90)$ were obtained for the other fissioning systems and used in the data analysis.

F. Calculation of the number of pre- and post-fission neutrons

The total number of neutrons $N_T(v_j,\theta)$ emitted per steradian per fission with a laboratory velocity v_j at an angle θ with respect to the fission-fragment direction is a sum of two components, the pre-fission neutrons $N_b(v_j,\theta)$ and the post-fission neutrons $N_a(v_j,\theta)$:

$$N_T(v_j,\theta)=N_b(v_j,\theta)+N_a(v_j,\theta)$$

with

$$N_a(v_j,\theta)=N_1(v_j,\theta)+N_2(v_j,\theta)\,, \tag{8}$$

where the subscript 1 and 2 stand for fragment No. 1 (detected at $\theta=0$) and fragment No. 2 (detected at $\theta=\pi$), respectively. We measured in our experiment the distributions $N_T(v_j,0)$, $N_T(v_j,\frac{1}{2}\pi)$, and $N_T(v_j,\pi)$. The relationship between these quantities and the quantities of interest, namely $N_b(v_j,\theta)$, $N_1(v_j,\theta)$ and $N_2(v_j,\theta)$ may be written in the form of these equations:

$$\begin{aligned}
N_1(v_j,0)&=N_T(v_j,0)-N_b(v_j,0)-N_2(v_j,0)\,,\\
N_2(v_j,\pi)&=N_T(v_j,\pi)-N_b(v_j,\pi)-N_1(v_j,\pi)\,,\\
N_b(v_j,\tfrac{1}{2}\pi)&=N_T(v_j,\tfrac{1}{2}\pi)-N_1(v_j,\tfrac{1}{2}\pi)-N_2(v_j,\tfrac{1}{2}\pi)\,.
\end{aligned} \tag{9}$$

[$N_i(v_j,\pi_j)$ are also functions of the fragment mass M and total fragment kinetic energy E_K, but for sake of clarity these subscripts are omitted in most equations.] In order to solve the above equations we make the following basic assumptions: (1) The pre-fission neutrons are emitted isotropically in the c.m. system of the compound nucleus. (2) The post-fission neutrons are emitted isotropically in the c.m. system of the fully accelerated fragments. (The validity of these assumptions is briefly discussed below.) With these assumptions Eqs. (9) can be solved and $N_b(v_j)$, $N_1(v_j)$ and $N_2(v_j)$ can be calculated. The average number of pre-fission and post-fission neutrons $\bar{\nu}_b(M,E_K)$ and $\bar{\nu}_a(M,E_K)$, respectively, is then obtained by a transformation to the c.m. frame of the fragments [for $\bar{\nu}_a(M,E_K)$] and a summation over $\bar{v}_j$:

$$\begin{aligned}
\bar{\nu}_b(M,E_K)&=\bar{\nu}_b(M_0-M,E_K)\\
&=\frac{4\pi}{Y(M,E_K)}\sum_{v_j}N_b(v_j,M,E_K)\,,\\
\bar{\nu}_a(M,E_K)&=\bar{\nu}_a(M_0-M,E_K)\\
&=\bar{\nu}_1(M,E_K)+\bar{\nu}_1(M_0-M,E_K)\,,\\
\bar{\nu}_1(M,E_K)&=\frac{4\pi}{Y(M,E_K)}\sum_{v_j}\left(1-\frac{V_1}{v_j}\right)^2N_1(v_j,0,M,E_K)\,,\\
\bar{\nu}_1(M_0-M,E_K)&=\frac{4\pi}{Y(M,E_K)}\sum_{v_j}\left(1-\frac{V_2}{v_j}\right)^2\\
&\quad\times N_2(v_j,\pi,M,E_K)\,.
\end{aligned} \tag{10}$$

Here $Y(M,E_K)=Y(M_0-M,E_K)$ is the fractional yield for the binary fission with fragment mass M and (M_0-M) and kinetic energy bin E_K:

$$\sum_M\sum_{E_K}Y(M,E_K)=1\,.$$

V_1 and V_2 are the velocities of fragments M and (M_0-M), respectively, and $(1-V_i/v_j)$ is the Jacobian of the laboratory to c.m. transformation.

We solved Eqs. (9) and (10) by an iteration method similar to that used by Cheifetz *et al.*[8] This method does not yield unique values for $\bar{\nu}_b$ and $\bar{\nu}_a$ but rather upper and lower limits which depend on the number of iterations performed. The method is described in greater detail in the Appendix.

G. Neutrons with kinetic energies outside the experimental detection limits

In the analysis of the pre-fission and post-fission neutrons we considered events in the velocity range of 0.95–4.55 cm/nsec (0.47–10.8 MeV). Above ~4.5 cm/sec the separation between neutrons and γ rays becomes uncertain. Below ~1.0 cm/nsec the background of random-coincidence events introduces increasingly larger errors and

the detection efficiency decreases rapidly because of the electronic threshold. The pre-fission neutrons are mainly affected by the low-velocity cutoff since their average kinetic energy is ~2 MeV. We estimate that ~7% of the pre-fission neutrons have velocities below our lower limit.[8] On the other hand the post-fission neutrons are mainly affected by the upper velocity cutoff. Based on considerations similar to those of Cheifetz *et al.*[8] we estimate that ~6% of the post-fission neutrons are above our velocity limit.

IV. EXPERIMENTAL RESULTS

The binary mass and kinetic energy distribution $Y(M, E_K)$ for the fragments prior to neutron emission were obtained for the various targets in a manner described in Sec. III. In Figs. 3–14, we show for these targets (a) the mass yield $Y(M) = \sum_{E_K} Y(M, E_K)$; (b) the total kinetic energy yield $Y(E_K) = \sum_M Y(M, E_K)$; (c) the average total kinetic energy as a function of fragment mass $\bar{E}_K(M) = \sum_{E_K} E_K Y(M, E_K)/Y(M)$. The average mass of the light and heavy fragments M_L and M_H, respectively, the standard deviation of the mass distribution $\sigma(M)$, the average $\bar{E}_K$, and the standard deviation $\sigma(E_K)$ of the total kinetic energy distribution are shown in Table II for all our targets.

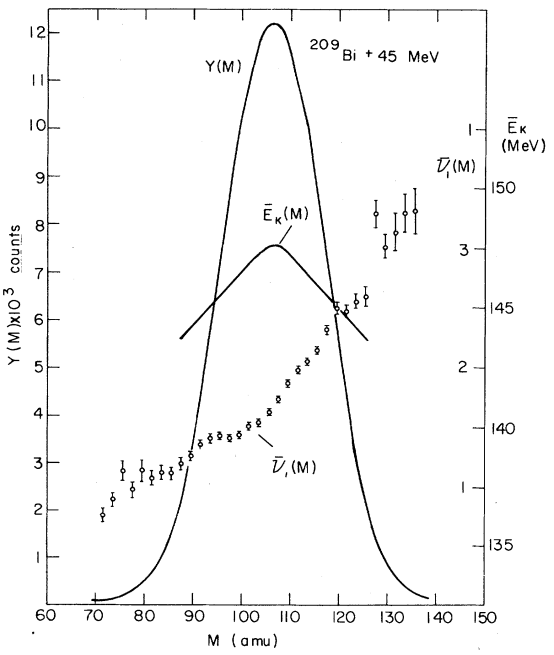

FIG. 3. The average number of post-fission neutrons $\bar{\nu}_1(M)$ and the average total fragment kinetic energy $\bar{E}_K(M)$ as a function of fragment mass M and the mass distribution $Y(M)$ for the system ^{209}Bi + 45 MeV α particles.

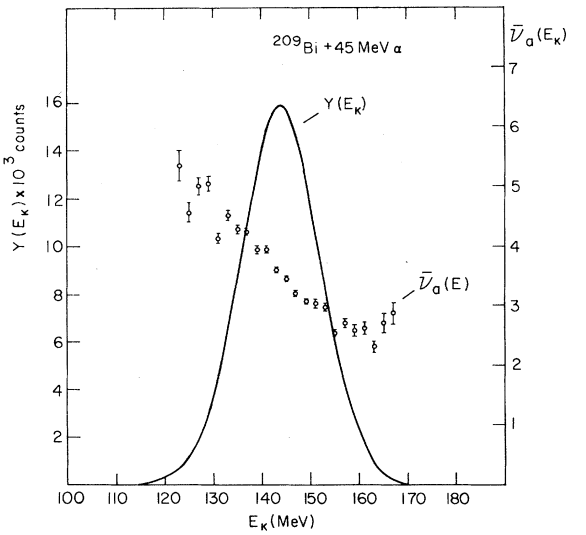

FIG. 4. The average number of post-fission neutrons from both fragments $\bar{\nu}_a(E_K)$ as a function of the total fragment kinetic energy E_K and the kinetic energy distribution $Y(E_K)$ for the system ^{209}Bi + 45 MeV α particles.

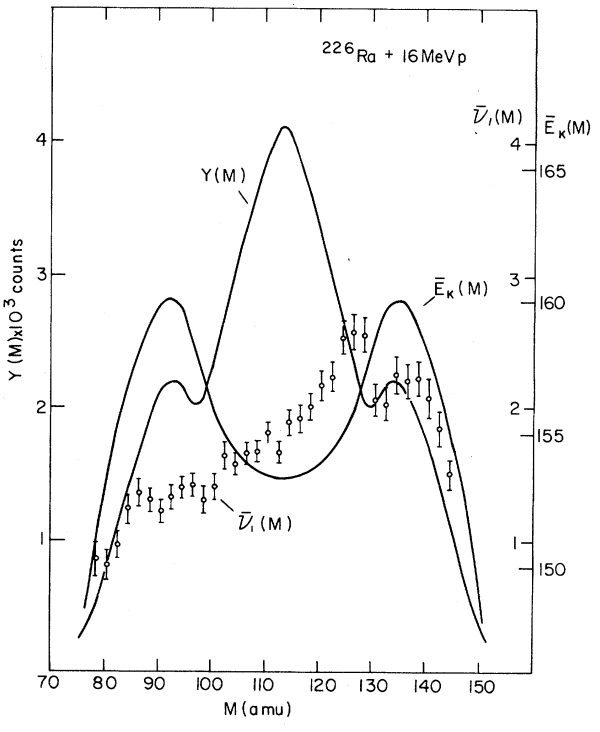

FIG. 5. The average number of post-fission neutrons $\bar{\nu}_1(M)$ and the average total fragment kinetic energy $\bar{E}_K(M)$ as a function of the fragment mass M and the mass distribution $Y(M)$ for the system ^{226}Ra + 16 MeV protons.

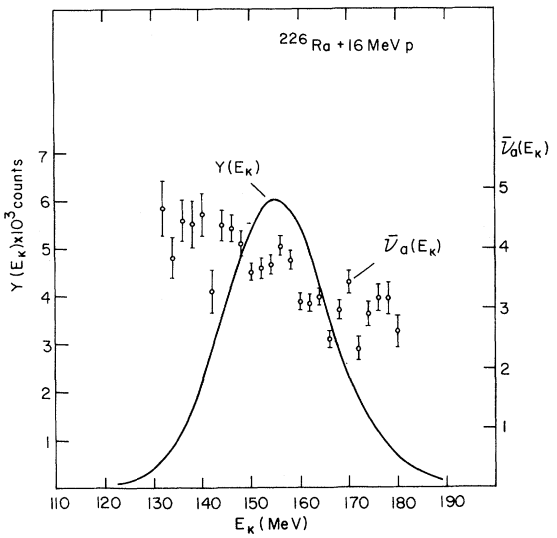

FIG. 6. The average number of post-fission neutrons from both fragments $\bar{\nu}_a(E_K)$ as a function of the total fragment kinetic energy E_K and the kinetic energy distribution $Y(E_K)$ for the system ^{226}Ra + 16 MeV protons.

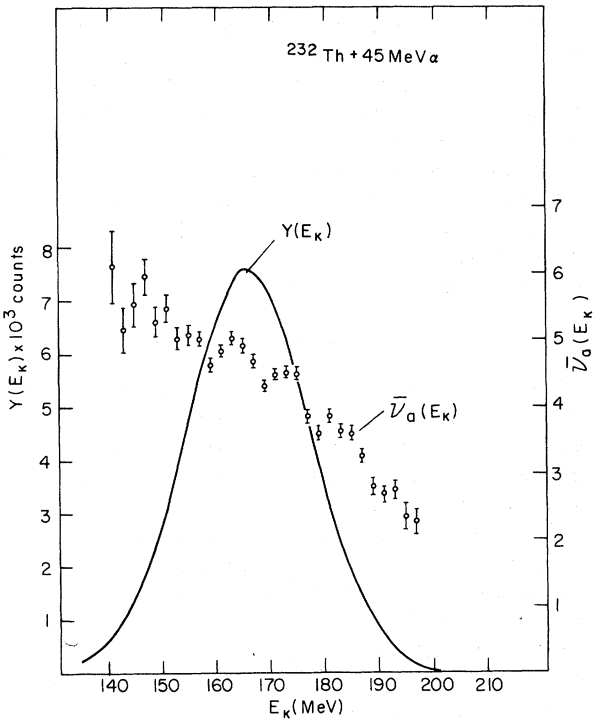

FIG. 8. The average number of post-fission neutrons from both fragments $\bar{\nu}_a(E_K)$ as a function of the total fragment kinetic energy E_K and the kinetic energy distribution $Y(E_K)$ for the system ^{232}Th + 45 MeV α particles.

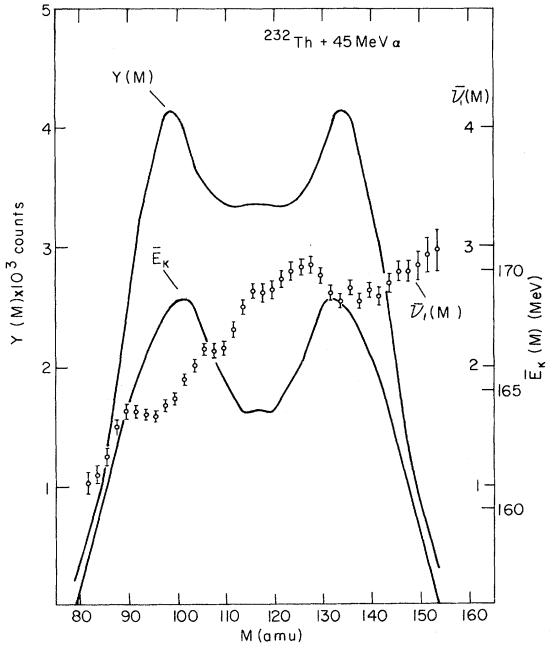

FIG. 7. The average number of post-fission neutrons $\bar{\nu}_1(M)$ and the average total fragment kinetic energy $\bar{E}_K(M)$ as a function of fragment mass M and the mass distribution $Y(M)$ for the system ^{232}Th + 45 MeV α particles.

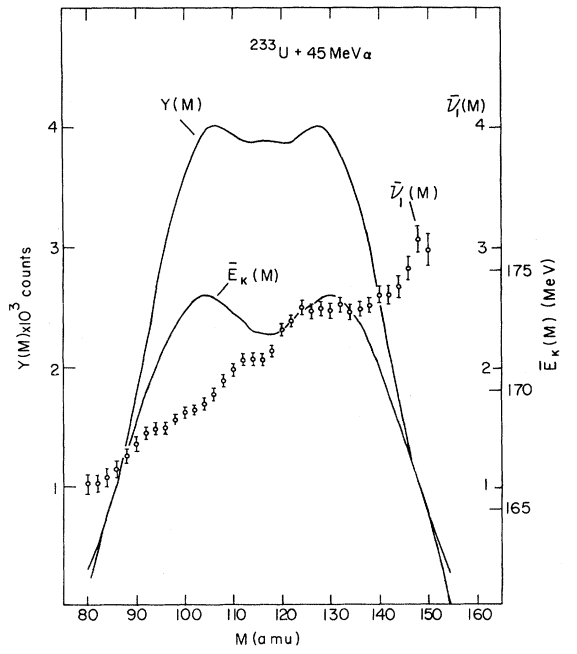

FIG. 9. The average number of post-fission neutrons $\bar{\nu}_1(M)$ and the average total fragment kinetic energy $\bar{E}_K(M)$ as a function of fragment mass M and the mass distribution $Y(M)$ for the system ^{233}U + 45 MeV α particles.

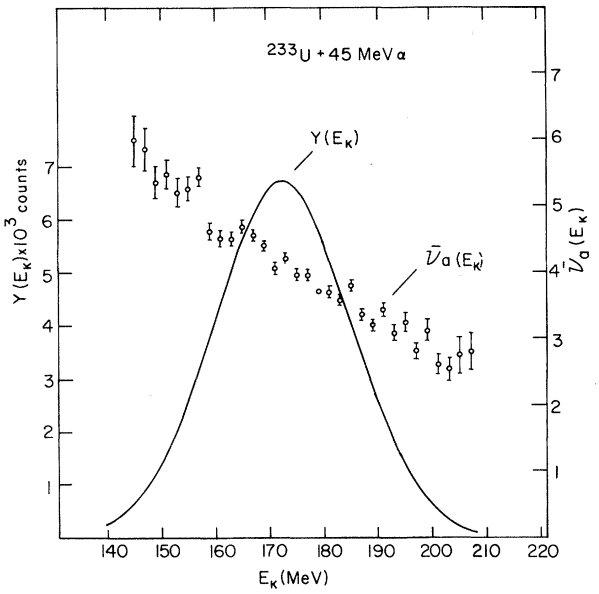

FIG. 10. The average number of post-fission neutrons from both fragments $\bar{\nu}_a(E_K)$ as a function of the total fragment kinetic energy E_K and the kinetic energy distribution $Y(E_K)$ for the system ^{233}U + 45 MeV α particles.

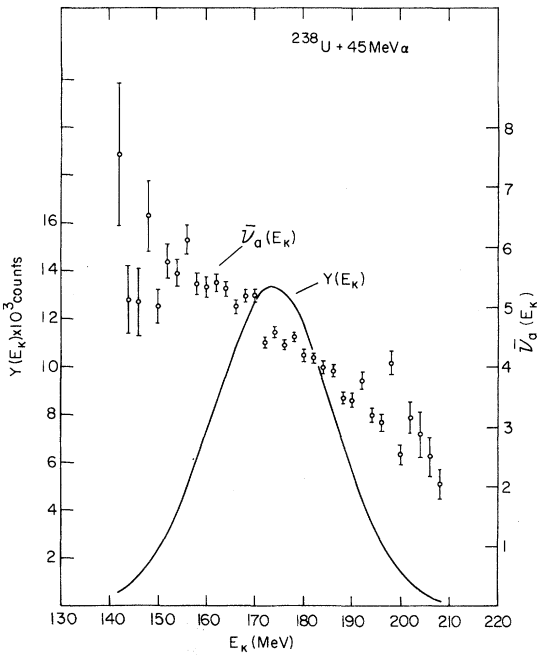

FIG. 12. The average number of post-fission neutrons from both fragments $\bar{\nu}_a(E_K)$ as a function of the total fragment kinetic energy E_K and the kinetic energy distribution for the system ^{238}U + 45 MeV α particles.

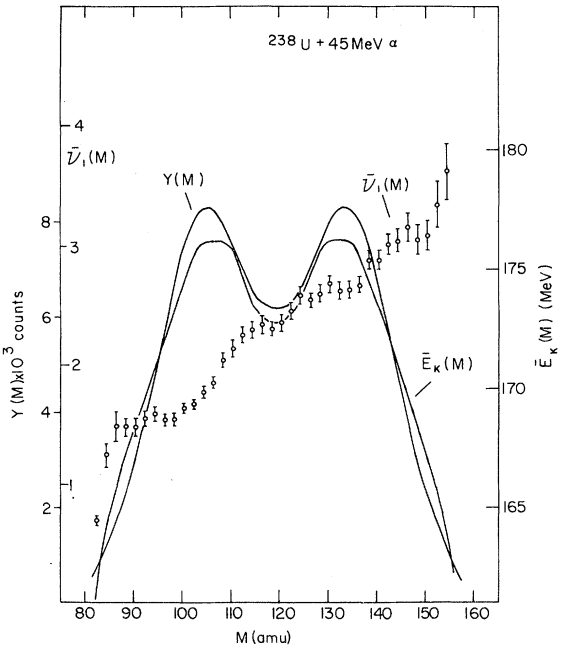

FIG. 11. The average number of post-fission neutrons $\bar{\nu}_1(M)$ and the average total fragment kinetic energy $\bar{E}_K(M)$ as a function of the fragment mass M and the mass distribution $Y(M)$ for the system ^{238}U + 45 MeV α particles.

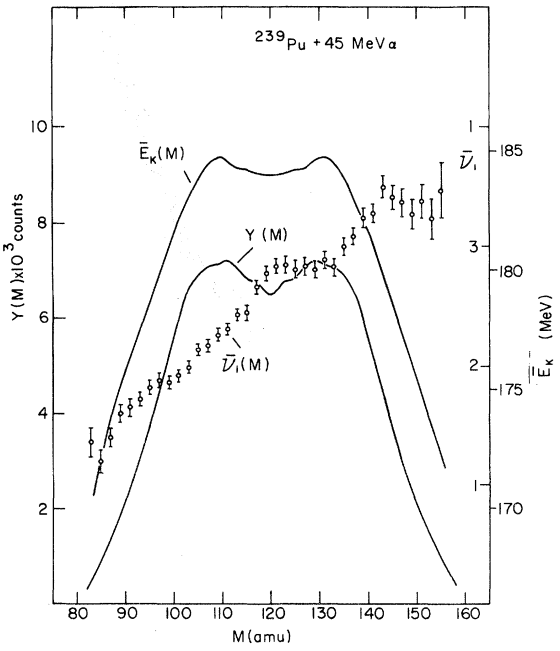

FIG. 13. The average number of post-fission neutrons $\bar{\nu}_1(M)$ and average kinetic energy $\bar{E}_K(M)$ as a function of the fragment mass M and the mass distribution $Y(M)$ for the system ^{239}U + 45 MeV α particles.

TABLE II. Characteristics of the binary fragment distribution $Y(M, E_K)$. The errors were estimated from differences between several measurements of the same quantities.

Compound nucleus	^{213}At	^{227}Ac	^{236}U	^{237}Pu	^{242}Pu	^{243}Cm
No. of events ($\times 10^4$)	16	8	11	10	21	18
$\overline{M}_L$ (amu)	98.4±0.5	99.7±0.5	100.9±0.5	102.9±0.5	104.5±0.5	105.8±0.5
$\overline{M}_H$ (amu)	114.6±0.5	127.3±0.5	132.1±0.5	131.1±0.5	134.5±0.5	134.2±0.5
σ_M (amu)	10.1±0.2	16.9±0.5	18.0±0.2	16.6±0.2	17.3±0.2	16.7±0.2
$\overline{E}_K$ (MeV)	146.0±1.0	156.0±1.0	166.0±1.0	172.4±1.0	174.0±1.0	182.5±1.0
σ_E (MeV)	8.0±0.2	11.2±0.2	11.3±0.3	12.1±0.3	12.0±0.4	12.8±0.4

In Table III we present the zeroth, first, and second moments [$N_T(\theta)$, $\overline{v}(\theta)$, and $\sigma_v(\theta)$, respectively] of the neutron laboratory velocity distribution as measured at $\theta = 0$ and 90°. These data pertain to the experimentally measured velocity interval of $0.95 \leq v(\theta) \leq 4.55$ cm/nsec. The errors shown are due to the uncertainty in the neutron detection efficiency.

We show in Figs. 3–14 the average number of post-fission neutrons as a function of the fragment mass and as a function of the total kinetic energy. $\overline{\nu}_1(M)$ denotes the average number of neutrons emitted from a fragment of mass M and $\overline{\nu}_a(E_K)$ denotes the average number of neutrons emitted from both fragments with total kinetic energy E_K. The curves are the mean between the upper and lower limits obtained in our iteration procedure. The errors shown are the statistical errors only.

We also obtained the number of pre-fission neutrons as a function of fragment mass ratio and total kinetic energy. Within the rather large errors (see also Table IV) the average number of pre-fission neutrons is independent of the mass ratio and of the total fragment kinetic energy.

In Table IV we show the upper and lower limits for the average number of pre-fission neutrons $\overline{\nu}_b$ and the average number of post-fission neutrons $\overline{\nu}_a$ as obtained with our iteration procedure. Also shown are the mean values for $\overline{\nu}_b$ and $\overline{\nu}_a$. In obtaining the mean values we took into account the error due to the effective efficiency and the correction due to the finite experimental velocity interval. Finally we also show in Table IV the average total number of neutrons emitted $\overline{\nu}_T = \overline{\nu}_b + \overline{\nu}_a$. Since the errors in $\overline{\nu}_b$ and $\overline{\nu}_a$ are correlated in our iteration procedure, the errors in $\overline{\nu}_T$ are smaller than would otherwise be the case.

V. CALCULATION OF THE NUMBER OF PRE-FISSION NEUTRONS

It was mentioned earlier that one of the main purposes of the present experiments was to see whether the conventional formulation for $\Gamma_f/\Gamma_n(E^*)$ can reproduce the experimental results for the average number of pre-fission neutrons and the radiochemical spallation residue cross sections for the reactions discussed in the present work (Table I). Such spallation residue cross sections have been measured for the actinide systems (^{232}Th, ^{233,238}U, ^{239}Pu + 45 MeV α) by Seaborg and co-workers.[20-22]

We have used the method of Dostrovsky *et al.*[9] to calculate the decay of the compound systems indicated in Table I. This method uses the Monte Carlo technique to calculate the decay of the compound nucleus by the evaporation of particles (mainly neutrons) and calculates at each evaporation step the fission probability using the expression for the ratio of fission width to neutron evap-

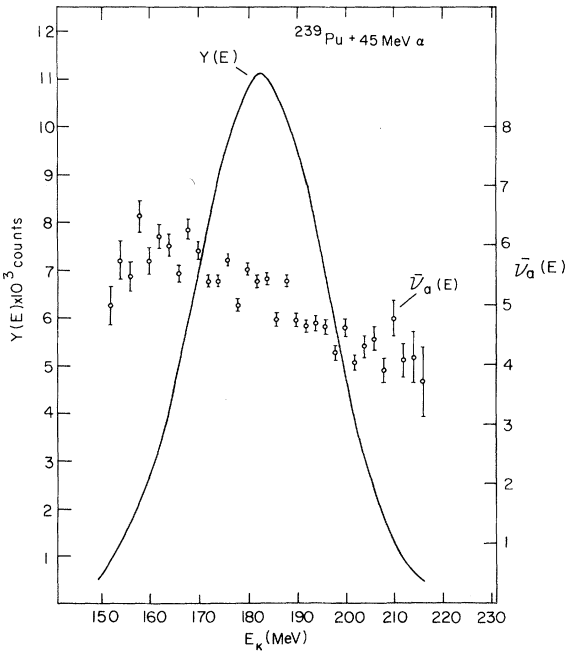

FIG. 14. The average number of post-fission neutrons from both fragments $\overline{\nu}_a(E_K)$ as a function of the total fragment kinetic energy E_K and the kinetic energy distribution for the system ^{239}Pu + 45 MeV α particles.

oration width[9,10]:

$$\frac{\Gamma_f}{\Gamma_n}=\frac{K_0 a_n\{2[a_f(E^*-B_f-\Delta_f)]^{1/2}-1\}}{4A^{2/3}a_f(E^*-B_n-\Delta_n)}$$
$$\times\exp\{2[a_f(E^*-B_f-\Delta_f)]^{1/2}$$
$$-2[a_n(E^*-B_n-\Delta_n)]^{1/2}\}\ . \qquad (11)$$

Here $K_0=\hbar^2/2mr_0^2\simeq 10$ MeV, a_n, and a_f are the level density parameters used in calculating the neutron emission and fission widths, respectively, E^* is the excitation energy of the compound nucleus, E_f is the fission barrier, B_n is the neutron binding energy, and Δ_n and Δ_f the respective shell plus pairing energy terms.

We have used for Δ_n the values tabulated by Cameron[23] and assumed[24] $\Delta_f(A,Z)+0.25$ MeV. [Note that in Eq. (11) Δ_f and Δ_n do not apply to the same A.] For the fission barrier heights B_f we used the experimental values shown in Table V and assumed $B_f=6.0$ MeV for all other $Z\geq 92$ nuclides. We used $B_f=8.5$ MeV for the Ac isotopes.[25]

The Monte Carlo calculation starts with the excited compound nucleus (Table I) and proceeds until the end of the evaporation cascade or until fission occurs. It thus yields among other results the pre-fission neutron distribution and the ratio of the fission cross section σ_F to the total reaction cross section σ_R (assuming σ_R to be equal to the compound nucleus formation cross section) and the ratio of any particular spallation cross section to the fission cross section.

We show in Table VI the calculated results for the average number of pre-fission neutrons $\bar{\nu}_b$, the ratio of the fission cross section to the total reaction cross section σ_F/σ_R, and the ratio of the $(\alpha,4n)$ spallation cross section to the fission cross section $\sigma(\alpha,4n)/\sigma_F$. The $(\alpha,4n)$ cross section is shown because it is the largest spallation cross section for our excitation energy range, according to the calculation. We also show in Table VI the experimental results (to the extent that they have been measured). The results for σ_F/σ_R and $\sigma(\alpha,4n)/\sigma_F$ were taken from the work of Seaborg and co-workers.[20-22] The calculated values of $\bar{\nu}_b$, σ_F/σ_R, and $\sigma(\alpha,4n)/\sigma_F$ are given for three sets of the level density parameters a_f and a_n: (1) $a_n=A/20$ and $a_f=\frac{4}{3}a_n=A/15$. A ratio of $a_f/a_n=1.2$–1.3 was found to apply in the lead region[24] (presumably because of the low level density in the ground state of the nuclei near the doubly closed shell). (2) $a_f=a_n=A/20$ and (3) $a_f=a_n=A/8$. For the nuclei of interest in the present work, which with the exception of the ^{209}Bi + α system are far from closed shells, one expects $a_f\simeq a_n$. The calculated results shown in Table VI have a statistical error (due to the Monte Carlo method) of ~0.01.

Comparing the calculated and experimental results for $\bar{\nu}_b$ we must keep in mind that our experimental results include scission neutrons whereas they are not included in the calculation. In order to obtain a quantitative estimate of the number of scission neutrons we analyzed the neutron distribution in the spontaneous fission of ^{252}Cf by the same method which we used to obtain the number of pre-fission and post-fission neutrons in the other fissioning systems. We found for ^{252}Cf $\bar{\nu}_b=0.4\pm0.1$, $\bar{\nu}_a=3.4\pm0.1$. This result is not independent of the results of Bowman *et al.*[12] which we used in our efficiency determination. They also estimated the number of scission neutrons to be ~0.4. Similar numbers were obtained by Cheifetz and Fraenkel[29] ($\bar{\nu}_b=0.25\pm0.20$). As a rough estimate we may assume 0.4 scission neutrons per fission for the other fissioning systems as well. (Loveland, Fairhall, and Halpern[30] found the number of scission α particles to be roughly independent of the fissioning species and excitation energy.) With this assumption most of the pre-fission neutrons of the system ^{226}Ra + 17 MeV

TABLE III. Characteristics of the neutron laboratory spectra in the velocity range $0.95<v<4.55$ cm/nsec at $\theta=0°$ and $\theta=90°$. The errors given are due to the uncertainty in the neutron detection efficiency. The error due to velocity dispersion is approximately 10%.

System	^{209}Bi + α	^{226}Ra + p	^{232}Th + α	^{233}U + α	^{238}U + α	^{239}Pu + α
No. of events (0°)	33 000	13 000	67 000	76 000	64 000	64 000
No. of events (90°)	•••	4000	33 000	44 000	36 000	29 000
$N_T(0°)$ (n/fission)	0.65 ± 0.02	0.69 ± 0.04	0.96 ± 0.02	1.02 ± 0.05	1.05 ± 0.05	1.06 ± 0.02
$N_T(90°)$ (n/fission)	•••	0.14 ± 0.02	0.38 ± 0.05	0.42 ± 0.08	0.46 ± 0.09	0.40 ± 0.04
$\bar{v}$ (0°) (cm/nsec)	2.06 ± 0.03	2.21 ± 0.03	2.26 ± 0.02	2.33 ± 0.02	2.31 ± 0.02	2.36 ± 0.02
$\bar{v}$(90°) (cm/nsec)	•••	1.86 ± 0.03	1.96 ± 0.06	2.01 ± 0.09	1.98 ± 0.08	2.01 ± 0.06
$\bar{E}_n$ (0°) (MeV)	2.42 ± 0.04	2.81 ± 0.03	2.97 ± 0.02	3.13 ± 0.04	3.08 ± 0.04	3.24 ± 0.04
$\bar{E}_n$ (90°) (MeV)	•••	2.03 ± 0.03	2.30 ± 0.12	2.40 ± 0.22	2.32 ± 0.22	2.42 ± 0.14
σ_v (0°) (cm/nsec)	0.62 ± 0.04	0.68 ± 0.02	0.75 ± 0.01	0.74 ± 0.01	0.74 ± 0.01	0.77 ± 0.01
σ_v (90°) (cm/nsec)	•••	0.66 ± 0.03	0.74 ± 0.03	0.75 ± 0.03	0.74 ± 0.05	0.77 ± 0.03

TABLE IV. The upper and lower limits of the number of pre-fission neutrons per fission $\bar{\nu}_b$ and number of post-fission neutrons per fragment $\bar{\nu}_1$ which result from the iteration for the velocity range $0.95 < v < 4.55$ cm/nsec, the average numbers of pre-fission neutrons $\bar{\nu}_b$, the average number of post-fission neutrons from both fragments $\bar{\nu}_a$, and the average total number of neutrons emitted per fission $\bar{\nu}_T$.

System	^{209}Bi + α	^{226}Ra + p	^{232}Th + α	^{233}U + α	^{238}U + α	^{239}Pu + α
$\bar{\nu}_b$ (upper)	•••	0.61 ± 0.15	3.72	4.79	5.13	3.42
$\bar{\nu}_b$ (lower)	•••	0.46 ± 0.15	2.02	1.88	2.10	1.89
$\bar{\nu}_b$	•••	0.5 ± 0.3	2.9 ± 0.9	3.3 ± 1.5	3.6 ± 1.6	2.7 ± 0.8
$\bar{\nu}_1$ (upper)	1.75 ± 0.05	1.76 ± 0.10	2.23	2.33	2.49	2.55
$\bar{\nu}_1$ (lower)	•••	1.74 ± 0.10	2.04	1.81	1.98	2.42
$\bar{\nu}_a$	3.6 ± 0.2	3.6 ± 0.4	4.4 ± 0.3	4.2 ± 0.7	4.6 ± 0.7	5.1 ± 0.3
$\bar{\nu}_T$	•••	4.1 ± 0.3	7.3 ± 0.8	7.5 ± 1.1	8.2 ± 1.1	7.8 ± 0.8

protons are scission neutrons and the number of "true" pre-fission neutrons is small or even zero.

Table VI shows that the calculated values for the average number of pre-fission neutrons $\bar{\nu}_b$ obtained with the set $a_f = A/15$, $a_n = A/20$ are very much smaller than the experimental values (except for ^{226}Ra + 17 MeV p). The calculated results for the sets $a_f = a_n = A/20$ and $a_f = a_n = A/8$ are in good agreement with the experimental results if 0.4 scission neutrons are added to the calculated results. In particular, the calculated results show no "true" pre-fission neutrons for ^{226}Ra + 17 MeV p. However, Table VI also shows a severe disagreement between the calculated results for $a_f = a_n = A/20$ and $a_f = a_n = A/8$ and the radiochemical results for σ_F/σ_R and $\sigma(\alpha, 4n)/\sigma_R$. The latter values are smaller by as much as three orders of magnitude than the calculated cross sections. This discrepancy will be briefly discussed below.

VI. DISCUSSION

A. Evaluation of the assumptions concerning neutron emission

In our analysis we made two assumptions regarding the angular distribution of the pre-fission and post-fission neutrons. We assumed: (1) that the pre-fission neutrons are emitted isotropically in the c.m. system of the compound nucleus; (2) that the post-fission neutrons are emitted isotropically in the c.m. system of the fully accelerated fragments. Our first assumption (regarding the pre-fission neutrons) would be in error if there is a sizeable forward-backward peaking of the neutron distribution in the c.m. system of the compound nucleus due to the angular momentum imparted to it by the incoming α particle. The result of the experiment of Drake, Axel, and Halpern[31] in which they bombarded Au with 42 MeV α particles and measured the angular distribution of the emitted neutrons shows this effect to be negligible for all our systems. Our second assumption (regarding the post-fission neutron distribution) raises two questions: (a) How large is the effect of the angular momentum of the fission fragment on the angular distribution of the emitted neutrons; (b) What is the probability of a neutron being emitted before the fragment is fully accelerated (the fragments have 99.9% of their final velocity $\sim 10^{-18}$ sec after scission)? Both these questions are discussed in detail by Cheifetz *et al.*[8] Based on their analysis we conclude that neutron emission prior to full fragment acceleration and angular momentum effects do not affect our results within our experimental error.

TABLE V. Fission barrier heights B_f (in MeV) used in the Γ_f/Γ_n calculation.

Z \ A	232	233	234	235	236	237	238	239	240	241	242	243
92	5.5[a]	5.7[b]	6.2[a]	6.1[c]	5.7[d]							
94						5.5[d]	6.0[d]	6.4[c]	5.8[a]	6.3[c]	6.3[d]	
96										5.9[d]	6.1[d]	5.9[d]

[a] Reference 26.
[b] Reference 25.
[c] Reference 27.
[d] Reference 28.

TABLE VI. The average number of pre-fission neutrons $\bar{\nu}_b$, the ratio of the fission cross section to the total reaction cross section σ_F/σ_R and the ratio of the $(\alpha, 4n)$ spallation cross section to the fission cross section $\sigma(\alpha,4n)/\sigma_F$ calculated for several values of the level density parameters a_f and a_n, and the experimental result. The error in the calculated results is ~0.01.

Fissioning system	$a_f = \frac{A}{15}$		$a_n = \frac{A}{20}$	$a_f = a_n = \frac{A}{20}$			$a_f = a_n = \frac{A}{8}$			Experimental		
	$\bar{\nu}_b$	$\frac{\sigma_F}{\sigma_R}$	$\frac{\sigma(\alpha,4n)}{\sigma_F}$	$\bar{\nu}_b$	$\frac{\sigma_F}{\sigma_R}$	$\frac{\sigma(\alpha,4n)}{\sigma_F}$	$\bar{\nu}_b$	$\frac{\sigma_F}{\sigma_R}$	$\frac{\sigma(\alpha,4n)}{\sigma_F}$	$\bar{\nu}_b$ [a]	$\frac{\sigma_F}{\sigma_R}$	$\frac{\sigma(\alpha,4n)}{\sigma_F}$
^{226}Ra + 17 MeV p	0.082	0.17		0.125	0.016		0	0.002		0.5 ± 0.2		
^{232}Th + 45 MeV α	0.039	1.00	0	2.73	0.68	0.40	2.68	0.92	0.045	2.9 ± 0.9		0.02 [b]
^{233}U + 45 MeV α	0.030	1.00	0	1.92	0.66	0.47	1.74	0.86	0.167	3.3 ± 1.5	~0.98 [c]	0.0002 [c]
^{238}U + 45 MeV α	0.066	1.00	0	2.81	0.52	0.73	2.82	0.81	0.102	3.6 ± 1.6		
^{239}Pu + 45 MeV α	0.063	1.00	0	2.32	0.79	0.23	2.18	0.94	0.51	2.7 ± 0.8	0.987 [d]	0.0004 [d]

[a] This work.

[b] Reference 22.

[c] Reference 21.

[d] Reference 20.

B. Comparison with other experimental results

There are at present no other direct measurements available of the number of pre-fission neutrons in our target-mass and excitation-energy range. But our results (Table IV) are consistent with the results of Cheifetz and Fraenkel[29] and of Bishop *et al.*[32,5] at lower excitation energies and with the results of Cheifetz *et al.*[8] at higher energies.

Our results for ^{209}Bi may be compared to the results of Plasil, Ferguson, and Schmitt[33] who bombarded ^{209}Bi with 52.25 MeV α particles. They obtained the number of neutrons as a function of fragment mass and total kinetic energy by measuring the kinetic energies of the two fragments and the velocity of one fragment. Their curve of $\bar{\nu}(M)$ is qualitatively similar to our results but both the slope of the curve and the absolute values for $\bar{\nu}(M)$ are much higher. Thus they obtain $\bar{\nu}_a = 7.4 \pm 0.5$ as compared to our value of 3.6 ± 0.2. They note that the former value is inconsistent with the total energy balance based on accepted mass formulas. A similar situation exists for the ^{226}Ra results. Here we compare our data with those of Konecny and Schmitt[34] who bombarded ^{226}Ra with 13 MeV protons and used the same method as Plasil *et al.*[33] to obtain $\bar{\nu}(M)$. The shape of their curve is similar to ours, in particular the relatively flat section in the mass region $M = 90$–100, the smooth increase in $\bar{\nu}(M)$ in the symmetric mass region $M = 100$–120, and the drop at $M \simeq 130$. But their experimental method yields higher values for $\bar{\nu}(M)$ than our direct neutron counting method in the mass region $M = 100$–130.

We can compare our results for $\nu_1(M)$ of ^{232}Th + 45 MeV α particles and ^{233}U + 45 MeV α particles with the early results of Britt and Whetstone.[35] They bombarded ^{230}Th, ^{232}Th, and ^{233}U with 22.1, 25.7, and 29.5 MeV α particles and measured the kinetic energy of the two fission fragments with solid state detectors. They obtained $\bar{\nu}_1(M)$ of ^{230}Th and ^{233}U for the bombarding energies of 25.7 and 29.5 MeV by comparing their results for the kinetic energies of the fragments with the results of Whetstone[36] who measured the velocity of the two fission fragments for the same fissioning systems using a time-of-flight technique. The method of Britt and Whetstone for the evaluation of $\bar{\nu}_1(M)$ suffers from the same basic difficulty as the method of Konecny and Schmitt[34] and Plasil *et al.*,[33] namely that a small number $[\bar{\nu}_1(M)]$ is obtained as the difference of two large numbers, namely the pre- and post-neutron emission fragment masses. As a result the relative error in $\bar{\nu}_1(M)$ is very much larger than the relative experimental error in measuring the two fragment mass distributions. Their results for $\bar{\nu}_1(M)$ of the system ^{230}Th + 29.5 MeV α particles are in good agreement with our results for ^{232}Th + 45 MeV α particles, but in view of the difference in the target mass and bombarding energy the agreement may be to some extent accidental. The results of Britt and Whetstone for ^{233}U + 29.5 MeV α particles are substantially higher than our values of $\bar{\nu}_1(M)$ for a bombarding energy of 45 MeV. The discrepancy may in part be due to an underestimate by Britt and Whetstone of the number of pre-fission neutrons emitted in this reaction (they assumed $\bar{\nu}_b = 0.15$).

C. Comparison with calculations and radiochemical results

We have presented results of calculations which assume Γ_f/Γ_n to be given by Eq. (11). Since we

used in these calculations the experimental fission barrier heights, a_f and a_n are the only "free" parameters in the calculation. It is seen from Table VI that good agreement with the experimental values for $\bar{\nu}_b$ is obtained within rather wide limits for $a_f = a_n = a$ ($a = A/8$ and $a = A/20$). The assumption that $a_f = a_n$ seems reasonable in our case since only near the closed shells is a_f expected to be substantially larger than a_n. Moreover, fits to the experimental level densities in the $Z = 92$–96 region yield $\sim A/10$ for both a_f and a_n.[28] We may thus conclude that the formulation of Γ_f/Γ_n as given by Eq. (11) reproduces satisfactorily our experimental results for the average number of pre-fission neutrons $\bar{\nu}_b$. However, the same calculations yield spallation cross sections which are larger, sometimes by orders of magnitude, than those measured by radiochemical methods. It was already mentioned that a similar discrepancy was found by Cheifetz *et al.*[8] for the fissioning systems of ^{238}U + 155 MeV p and ^{209}Bi + 155 MeV p. But whereas in the case of Cheifetz *et al.* the spallation-fission calculation is "complicated" by the intranuclear fast cascade which precedes the fission-neutron evaporation mechanism, this is not true in the present work. It may also be of interest to mention in this context the recent work of Boyce *et al.*[37] They measured very accurately the absolute cross section for 5.0–30.0 MeV proton-induced fission in various uranium isotopes. They compared their experimental results with calculations which use an expression for Γ_f/Γ_n which is similar to Eq. (11) and an optical model calculation to obtain the total reaction cross section. They obtained fairly good agreement with their experimental results. (However, they found it necessary to multiply all reaction cross sections by an energy dependent factor, presumably because of the shortcomings of the optical model calculations.)

In summary it should be emphasized that while it does not seem that agreement can be obtained between the results of the present experiment and the radiochemical spallation results using a formulation for Γ_f/Γ_n as given by Eq. (11), the two sets of experimental results are not inherently incompatible. A more realistic calculation of the fission-spallation competition may eliminate the present disagreement. A calculation of this kind is in progress.

ACKNOWLEDGMENT

The experimental work described in this paper was done while two of the authors (Z. F., W. L.) were guests of the Chemistry Division of the Argonne National Laboratory. They wish to express their sincere thanks for its hospitality. The calculations were done while Z. F. was a guest at the Lawrence Berkeley Laboratory. He wishes to thank Dr. S. G. Thompson, Professor L. G. Moretto, and the Nuclear Chemistry Division for their hospitality. We thank Dr. A. Gavron and Dr. E. Cheifetz for their valuable help in the analysis of the experimental results and for many useful discussions.

APPENDIX

In this Appendix we describe how the number of neutrons $\bar{\nu}_b(M, E_K)$ and $\bar{\nu}_a(M, E_K)$ were obtained from the experimental quantities $N_T(v_j, 0)$, $N_T(v_j, \frac{1}{2}\pi)$, and $N_T(v_j, \pi)$. Equations (9) may be rewritten in the form

$$N_1(v_j, 0) = N_T(v_j, 0) - N_b(v_j) - T_\delta(2, j) N_2(v_{l2}, \pi) ,$$

$$N_2(v_j, \pi) = N_T(v_j, \pi) - N_b(v_j) - T_\delta(1, j) N_1(v_{l1}, 0) , \quad \text{(A1)}$$

$$N_b(v_j) = N_T(v_j, \tfrac{1}{2}\pi) - \sum_{i=1}^{2} T_\beta(i, j) N_i(v_{ki}, \theta_i) ,$$

where $\theta_1 = 0$ and $\theta_2 = \pi$. For reasons of symmetry $N_b(v_j)$ has no θ dependence and hence, no assumption regarding the pre-fission neutron distribution is needed to solve Eq. (A1) and to obtain the post-fission neutron distribution $N_i(v_j)$. Assuming the post-fission neutrons to be emitted isotropically from the fully accelerated fragments we obtain the following simple expressions for the transformation matrices:

$$T_\beta(i, j) = \left(1 - \frac{2V_i}{v_{ki}}\right)^{1/2} \left(1 - \frac{V_i}{v_{ki}}\right) ,$$

$$T_\delta(i, j) = \left(1 - \frac{2V_i}{v_{li}}\right)^2 , \quad \text{(A2)}$$

$$v_{ki} = V_i + (V_i^2 + v_j^2)^{1/2} ,$$

$$v_{li} = 2V_i + v_j ,$$

where V_i is the velocity of fragment i. Equations (A1) can, in principle, be solved analytically. However, it is simplier to solve them by expansion in powers of $T(i, j)$, as was done by Cheifetz *et al.*[8] The expansion converges rapidly since $T(i, j) < 1$ [see Eq. (A2)] and higher terms of the expansion operate on higher velocity components of $N_T(v_j, \theta)$ which is a rapidly decreasing function of v_j. Moreover, our measurements were limited to the velocity range $1.0 \leq v_j \leq 4.5$ cm/nsec.

To first order in $T(i, j)$

TABLE VII. The contribution of a neutron event with laboratory velocity v_j detected at $\theta = 0$ to the moments of the pre-fission and post-fission neutron velocity distributions. $v^{(n)}$ is the nth moment of the velocity distribution. M is the mass of the fragment detected at $\theta = 0$, $M_0 - M$ is the mass of the complementary fragment (detected at $\theta = \pi$).

Moment of velocity distribution	Contributing fraction of one neutron event	Velocity limits other than $4.55 > v_j > 0.95$ cm/nsec
$v_1^{(n)}(M, E_K)$	$(v_j - V_1)^n \left(1 - \frac{V_1}{v_j}\right)^2 N_T'(v_j, 0)$	$v_j > V_1$
	$+ \frac{[(v_j^2 - 2v_jV_1)^{1/2} - V_1]^{n+2}}{(v_j^2 - 2v_jV_1)} T_\beta(1,j) N_T'(v_j, 0)$	$v_j > (1+\sqrt{2})V_1$ $(v_j^2 - 2v_jV_1)^{1/2} > 0.95$ cm/nsec
$v_1^{(n)}(M_0 - M, E_K)$	$\frac{[(v_j^2 - 2v_jV_1)^{1/2} - V_2)]^{n+2}}{(v_j^2 - 2v_jV_1)} T_\beta(1,j) N_T'(v_j, 0)$	$v_j > V_1 + (V_1^2 + V_2^2)^{1/2}$ $(v_j^2 - 2v_jV_1)^{1/2} > 0.95$ cm/nsec
	$- \frac{(v_j - 2V_1 - V_2)^{n+2}}{(v_j - 2V_1)^2} T_\delta(1,j) N_T'(v_j, 0)$	$v_j > 2V_1 + V_2$ $(v_j - 2V_1) > 0.95$ cm/nsec
$v_b^{(n)}(E_K)$	$-(v_j^2 - 2v_jV_1)^{n/2} T_\beta(1,j) N_T'(v_j, 0)$	$v_j > 2V_1$ $(v_j^2 - 2v_jV_1)^{1/2} > 0.95$ cm/nsec
	$T_\beta(1,j) = \left(1 - \frac{2V_1}{v_j}\right)^{1/2} \left(1 - \frac{V_1}{v_j}\right)$	
	$T_\delta(1,j) = \left(1 - \frac{2V_1}{v_j}\right)^2$	

$$N_1(v_j, 0) = N_T(v_j, 0) - N_T(v_j, \tfrac{1}{2}\pi) + T_\beta(1,j)[N_T(v_{k1}, 0) - N_T(v_{k1}, \tfrac{1}{2}\pi)] + T_\beta(2,j)[N_T(v_{k2}, \pi) - N_T(v_{k2}, \tfrac{1}{2}\pi)]$$
$$- T_\delta(2,j)[N_T(v_{l2}, \pi) - N_T(v_{l2}, \tfrac{1}{2}\pi)] \,, \qquad \text{(A3)}$$
$$N_b(v_j) = N_T(v_j, \tfrac{1}{2}\pi) - \sum_{i=1}^{2} T_\beta(i,j)[N_T(v_{ki}, \theta_i) - N_T(v_{ki}, \tfrac{1}{2}\pi)] \,.$$

The equation for $N_2(v_j, \pi)$ is obtained from the equation for $N_1(v_j, 0)$ by interchanging the angles 0 and π and the subscripts 1 and 2.

In contrast to the method used by Cheifetz *et al.*[8] in which the detected events were initially sorted into three-dimensional arrays corresponding to M, E_K, and v_j for $\theta = 0$, $\frac{1}{2}\pi$, and π and the iteration procedure was later carried out on these arrays, we performed the analysis event by event prior to any sorting, thereby eliminating the dispersion effects introduced by the initial sorting procedure. We tabulate in Table VII, as an example, the contribution of an event in which a neutron of velocity v_j is detected at $\theta = 0°$ to the moments of the pre-fission and post-fission neutron velocity distribution. $N_T'(v_j, \theta) = [N_0 \epsilon(v_j, \theta)\Omega]^{-1}$ is the weight of one neutron event. Ω is the solid angle of the neutron detector.

In carrying out the iteration procedure to first order [Eq. (A3)], we obtain an upper limit for $\bar{\nu}_b$ and a lower limit for $\bar{\nu}_a$.[8] By omitting the $N_T(V_{ki}, \frac{1}{2}\pi)$ terms from Eq. (A3), we obtain a lower limit for $\bar{\nu}_b$ and an upper limit for $\bar{\nu}_a$. The differences between these limits can, in principle, be reduced by adding higher order terms to Eq. (A3). In practice, other uncertainties, and in particular, the errors in $\epsilon(v_j, \theta)$ are of the same order as the difference between the upper and lower limits of the first order iteration and hence, the inclusion of higher terms is not useful, and our results show the upper and lower limits for $\bar{\nu}_b$ and $\bar{\nu}_a$ as obtained from the first-order iteration.

Since post-fission neutrons with laboratory energy of 4.5 cm/nsec at 0° have the same c.m. energy as a 3.1 cm/nsec post-fission neutron at 90° and a ~2.1 cm/nsec neutron at 180°, the iteration procedure cannot be carried out even to first order on T_β and T_δ above these limits (see Table VII). The effect of the limits on the T_δ terms on the final results is negligible since these terms are very small. However, the effect of the limits of the T_β term results in overestimating of $\bar{\nu}_b$ by 0.06 ± 0.06 neutrons per fission and underestimating of $\bar{\nu}_a$ by 0.04 ± 0.04 neutrons per fission.

†Permanent address: Weizmann Institute of Science, Rehovot, Israel.
‡Permanent address: Oregon State University, Corwallis, Oregon.
*Work supported in part by the U.S. Atomic Energy Commission.

[1]A. Khodai-Joopari, Lawrence Radiation Laboratory Report No. UCRL-16489, 1966 (unpublished).
[2]G. M. Raisbeck and J. W. Cobble, Phys. Rev. 153, 1270 (1967).
[3]L. G. Moretto, S. G. Thompson, J. Routti, and R. C. Gatti, Phys. Lett. 38B, 471 (1972).
[4]R. Vandenbosch and U. Mosel, Phys. Rev. Lett. 28, 1726 (1972).
[5]C. J. Bishop, I. Halpern, R. W. Shaw, Jr., and R. Vandenbosch, Nucl. Phys. A198, 161 (1972).
[6]H. Freiesleben, H. C. Britt, and J. R. Huizenga, in *Proceedings of the Third International Atomic Energy Agency Symposium on the Physics and Chemistry of Fission, Rochester, 1973* (International Atomic Energy Agency, Vienna, 1974), Vol. I, p. 447.
[7]L. G. Moretto, in *Proceedings of the Third International Atomic Energy Agency Symposium on the Physics and Chemistry of Fission, Rochester, 1973* (see Ref. 6), Vol. I, p. 329. (See this review paper for earlier references.
[8]E. Cheifetz, Z. Fraenkel, J. Galin, M. Lefort, J. Peter, and X. Tarrago, Phys. Rev. C 2, 256 (1970).
[9]I. Dostrovsky, Z. Fraenkel, and P. Rabinovitch, in *Proceedings of the Second United Nations International Conference on the Peaceful Uses of Atomic Energy* (United Nations, Geneva, 1958), Vol. 15, p. 301.
[10]J. R. Huizenga and R. Vandenbosch, in *Nuclear Reactions*, edited by P. M. Endt and P. B. Smith (North-Holland, Amsterdam, 1962), Vol. II.
[11]G. N. Harding and F. J. M. Farley, Proc. Phys. Soc. (Lond.) A69, 853 (1956).
[12]H. R. Bowman, S. G. Thompson, J. C. D. Milton, and W. J. Swiatecki, Phys. Rev. 126, 2120 (1962).
[13]J. C. D. Milton and J. S. Fraser, in *Proceedings of the First International Symposium on the Physics and Chemistry of Fission, Salzburg, Austria, 1965* (International Atomic Energy Agency, Vienna, 1965), Vol. II, p. 39.
[14]S. W. Cosper, J. Cerny, and R. C. Gatti, Phys. Rev. 154, 1193 (1967).
[15]A. Gavron, Nucl. Instrum. Methods 115, 99 (1974).
[16]H. R. Bowman, J. C. D. Milton, S. G. Thompson, and W. J. Swiatecki, Phys. Rev. 129, 2133 (1963).
[17]H. W. Schmitt, W. E. Kiker, and C. W. Williams, Phys. Rev. 137, B837 (1965).
[18]R. L. Watson, J. B. Wilhelmy, R. C. Jared, C. Rugge, H. R. Bowman, S. G. Thompson, and J. O. Rasmussen, Nucl. Phys. A141, 449 (1970).
[19]M. E. Rose, Phys. Rev. 91, 610 (1953).
[20]R. A. Glass, J. J. Carr, J. W. Cobble, and G. T. Seaborg, Phys. Rev. 104, 434 (1956).
[21]R. Vandenbosch, T. D. Thomas, S. E. Vandenbosch, R. A. Glass, and G. T. Seaborg, Phys. Rev. 111, 1358 (1958).
[22]B. M. Foreman, W. M. Gibson, R. A. Glass, and G. T. Seaborg, Phys. Rev. 116, 382 (1959).
[23]A. G. W. Cameron, Can. J. Phys. 36, 1940 (1958).
[24]R. Vandenbosch and J. R. Huizenga, *Nuclear Fission* (Academic, New York, 1973), Chap. VII.
[25]See Ref. 24, Table VIII-1.
[26]B. B. Back, O. Hansen, H. C. Britt, and J. D. Barrett, in *Proceedings of the Third International Atomic Energy Agency Symposium on the Physics and Chemistry of Fission, Rochester, 1973* (see Ref. 6), Vol. I, p. 25.
[27]B. B. Back, H. C. Britt, J. D. Garrett, and B. Leroux, in *Proceedings of the Third International Atomic Energy Agency Symposium on the Physics and Chemistry of Fission, Rochester, 1973* (see Ref. 6), Vol. I, p. 3.
[28]A. Gavron and H. C. Britt (private communication).
[29]E. Cheifetz and Z. Fraenkel, Phys. Rev. Lett. 21, 36 (1968).
[30]W. D. Loveland, A. E. Fairhall, and I. Halpern, Phys. Rev. 163, 1315 (1967).
[31]D. M. Drake, P. Axel, and I. Halpern, in *Proceedings of the Conference on Direct Interactions and Nuclear Reaction Mechanisms, Padua, Italy, 1962*, edited by E. Clementel and C. Villi (Gordon and Breach, New York, 1963).
[32]C. J. Bishop, R. Vandenbosch, R. Aley, R. W. Shaw, Jr., and I. Halpern, Nucl. Phys. A150, 129 (1970).
[33]F. Plasil, R. L. Ferguson, and H. W. Schmitt, in *Proceedings of the Second International Atomic Energy Agency Symposium on the Physics and Chemistry of Fission, Vienna, Austria, 1969* (International Atomic Energy Agency, Vienna, 1969), p. 505.
[34]E. Konecny and H. W. Schmitt, Phys. Rev. 172, 1213 (1968).
[35]H. C. Britt and S. L. Whetstone, Jr., Phys. Rev. 133, B603 (1969).
[36]S. L. Whetstone, Jr., Phys. Rev. 133, B613 (1964).
[37]J. R. Boyce, T. D. Hayword, R. Boss, H. W. Newson, E. G. Bilpuch, F. D. Purser, and H. W. Schmitt, Phys. Rev. C 10, 231 (1974).